Impurity-induced localization of Bose–Einstein condensates in one-dimensional optical lattices*

Wang Jian-Jun(王建军)[a)b)], Zhang Ai-Xia(张爱霞)[a)], and Xue Ju-Kui(薛具奎)[a)†]

[a)] *Key Laboratory of Atomic & Molecular Physics and Functional Materials of Gansu Province, College of Physics and Electronics Engineering, Northwest Normal University, Lanzhou* 730070, *China*

[b)] *Gansu Provincial Library, Lanzhou* 730000, *China*

(Received 25 January 2011; revised manuscript received 29 March 2011)

The impurity-induced localization of two-component Bose–Einstein condensates loaded into deep one-dimensional optical lattices is studied both analytically and numerically. It is shown that, the analytical criteria for self-trapping and moving soliton/breather of the primary-component condensate are modified significantly by an admixture of an impurity component (the second component). The realization of the self-trapped state and the moving soliton/breather states of the primary-component becomes more easy with the minor admixture of the impurity-component, even if the two components are partly overlapped.

Keywords: two-component, optical lattices, self-trapping, moving soliton/breather

PACS: 03.75.Kk, 03.75.Mn, 03.75.Lm **DOI:** 10.1088/1674-1056/20/8/080308

1. Introduction

Two-component Bose–Einstein condensates (BECs) have rich and novel types of phase transition and nonlinear localization of coherent matter waves.[1−5] A prominent experiment has demonstrated the superfluid-Mott-insulator transition[6] and Fermionic superfluid in the BEC-BCS crossover regime.[7,8] Then, experiments with a hetero-nuclear mixture in three-dimensional (3D) optical lattices have realized a Fermi–Bose system.[9,10] In particular, a new investigation of degenerate Bose–Bose mixtures in an optical lattice has again opened up uncharted territory.[11] In these experiments, the loss of phase coherence of the primary-component, ^{87}Rb, is enriched due to an admixture of the second component (considered as an impurity), ^{41}K, not only for the minor component, but even for the marginal spatial overlap between the two components. Recently, our theoretical study[12] revealed that the presence of the second component can significantly modify the coherent dynamics of the primary component and leads to a lot of interesting quantum phenomena of the two-component condensates.

This paper extends our recent work[12] and focuses on discussing the impurity-induced localization of two-component BECs in one-dimensional (1D) optical lattices. Based on a discrete Gross–Pitaevskii equation (GPE) and within a time-dependent variational approach, we obtain the analytical criteria of the self-trapping and the moving soliton/breather of the primary component in a Bose–Bose mixture system, especially for a moving Bose–Bose mixture system. Our analytical results are confirmed by the direct numerical simulations of the discrete GPE, with two same and two different components, ^{87}Rb (the primary component) and ^{41}K (the second component). It shows that the critical conditions for occurrences of the self-trapped state and the moving soliton/breather states can be modified significantly by an admixture of an impurity (i.e., the second component). The realization of these located states becomes easier with the minor admixture of the impurity component, even if the two components are partly overlapped. Furthermore, a new moving soliton state is found in this paper. All results reveal that the impurity plays a key role in manipulating and controlling the coherent dynamics of the two-component condensates.

*Project supported by the National Natural Science Foundation of China (Grant Nos. 10774120 and 10975114), the Natural Science Foundation of Gansu Province of China (Grant No. 1010RJZA012), and the Natural Science Foundation of Northwest Normal University of China (Grant No. NWNU-KJCXGC-03-48).

†Corresponding author. E-mail: xuejk@nwnu.edu.cn

© 2011 Chinese Physical Society and IOP Publishing Ltd

2. Model

Under the mean-field theory, the dynamics of two-component BECs loaded into 1D untilted optical lattices at $T = 0$ satisfies the GPE:[12]

$$\mathrm{i}\frac{\partial \Psi^l}{\partial t} = \left[-\beta_l \frac{\partial^2}{\partial x^2} + V(x) + \sum_{j=1}^{2} g_{lj}|\Psi^j|^2\right]\Psi^l, \quad (1)$$

where time and space have been rescaled as $t \sim tE_{\mathrm{R}}^1/\hbar$ and $x \sim \kappa x$, respectively, l, j ($l \neq j$) represent the different components, Ψ^l is the wave function of the l-th component. The nonlinear coefficients, corresponding to the intra-component atoms interaction ($l = j$) and the inter-component atoms interaction ($l \neq j$) are given in terms of the scattering length a_{lj} by $g_{ll} = 4\pi\hbar^2 a_{ll}/E_{\mathrm{R}}^1 M_l$ and $g_{lj} = 2\pi\hbar^2 a_{lj}(M_l + M_j)/E_{\mathrm{R}}^1 M_l M_j$, with M_l being the mass of one atom of the l-th component. The $V(x) = s\cos(2x)$ is the external optical lattice potential created by one orthogonal pair of counter-propagating laser beams, s is the strength of the optical lattices, $E_{\mathrm{R}}^l = \hbar^2\kappa^2/2M_l$ is the recoil energy of the lattices, κ is the wave number of the laser beams and $\beta_l = M_1/M_l$. When we consider the admixture of two different components, i.e., ^{87}Rb (the primary component) and ^{41}K (the second component), as used in experiment,[11] $\beta_1 = 1$ and $\beta_2 = 2.19$.

When the optical lattices are sufficiently deep, we can work within the tight-binding limit. In this case, the l-th condensate wave-function can be written as $\Psi^l(x,t) = \sqrt{N_l}\sum_n \Psi_n^l(t)\phi^l(x - x_n)$, where N_l is the total number of atoms of the l-th component, $\Psi_n^l(t)$ is the n-th amplitude and $\phi^l(x - x_n)$ is the Wannier function of the lowest band localized at site n, with the normalization condition $\int \mathrm{d}x(\phi_n^l)^2 = 1$ and the orthogonalization condition $\int \mathrm{d}x\phi_n^l\phi_{n+1}^l \simeq 0$. Inserting the above tight-binding approximation into the GPE Eq. (1), and integrating over the spatial degree of freedom using the re-scaled time $t \sim 2K_1 t$, we obtain the following discrete GPE:

$$\begin{aligned}\mathrm{i}\frac{\partial \Psi_n^l}{\partial t} &= -\frac{\beta_l}{2}(\Psi_{n-1}^l + \Psi_{n+1}^l) \\ &\quad + (\Lambda_{ll}|\Psi_n^l|^2 + \Lambda_{lj}|\Psi_n^j|^2)\Psi_n^l, \end{aligned} \quad (2)$$

where

$$K_l \simeq -\int \mathrm{d}x[\nabla\phi_{n+1}^l \nabla\phi_n^l + s\cos(2x)\phi_{n+1}^l\phi_n^l]$$

represents the tunneling between the adjacent sites of the l-th component. The nonlinear coefficients

$$\Lambda_{ll} = 2\pi\hbar^2 a_{ll}N_l/K_1 E_{\mathrm{R}}^1 M_l \int \mathrm{d}x|\phi_n^l|^4$$

and

$$\Lambda_{lj} = \frac{\pi\hbar^2 a_{lj}N_j(M_l + M_j)}{E_{\mathrm{R}}^1 K_1 M_l M_j}\int \mathrm{d}x|\phi_n^l|^2|\phi_n^j|^2 = \lambda_l\Lambda_{ll}$$

represent the intra-component and inter-component atoms interactions, respectively. Here, we only consider the repulsive atoms interaction for the intra-component ($\Lambda_{ll} > 0$). According to Refs. [13] and [14], Λ_{ll} and λ_l can be estimated analytically: $\Lambda_{ll} = 2^{-5/2}\pi\hbar^2 a_{ll}N_l s^{-1/2}\,\mathrm{e}^{2\sqrt{s}}/E_{\mathrm{R}}^1 M_l d a_\perp^2$, $\lambda_l = a_{lj}N_j(M_l + M_j)/2a_{ll}N_l M_j$, where d is the lattice period and $a_\perp$ is the transverse trapping length. Equation (2) can be written as $\dot{\Psi}^l{}_n = \partial H_l/\partial[\mathrm{i}(\Psi_n^l)^*]$, where H_l is the Hamiltonian of the l-th component

$$\begin{aligned}H_l = \sum_n \Big\{ &-\frac{\beta_l}{2}[(\Psi_n^l)^*\Psi_{n+1}^l + \Psi_n^l(\Psi_{n+1}^l)^*] \\ &+ \frac{\Lambda_{ll}}{2}(|\Psi_n^l|^2 + 2\lambda_l|\Psi_n^j|^2)|\Psi_n^l|^2\Big\}. \end{aligned} \quad (3)$$

3. The time-dependent variational analysis

To study the dynamics of the two-component BECs trapped into 1D deep optical lattices, we consider the evolution of two Gaussian profile wave packets:

$$\begin{aligned}&\Psi_n^l(t) \\ &= \frac{1}{\sqrt[4]{\pi/2}\sqrt{R_l}} \\ &\quad \times \exp\left[-\frac{(n-\xi_l)^2}{R_l^2} + \mathrm{i}p_l(n-\xi_l) + \mathrm{i}\frac{\delta_l}{2}(n-\xi_l)^2\right]. \end{aligned}$$

The $\xi_l(t)$ and $R_l(t)$ are the centre and the width of the l-th component wave packet, respectively, $p_l(t)$ and $\delta_l(t)$ are their associated momenta, respectively. The dynamical evolution of the wave packet can be obtained by a variational principle from the Lagrangian $L_l = \sum_n \mathrm{i}[\dot{\Psi}^l{}_n(\Psi_n^l)^* - \Psi_n^l(\dot{\Psi}^l{}_n)^*] - H_l$, with equations of motion for the variational parameters $q_l(t) = \xi_l(t)$, $R_l(t)$, $p_l(t)$, $\delta_l(t)$ given by

$$\frac{\mathrm{d}}{\mathrm{d}t}\frac{\partial L_l}{\partial \dot{q}_l} = \frac{\partial L_l}{\partial q_l},$$

where H_l is given by Eq. (3). In our calculation, we replace the sum over n in the Lagrangian by the integral when R_l is not too small.[12–14] All these parameters lead to

$$L_l = 2p_l\dot{\xi}_l - \frac{1}{4}\dot{\delta}_l R_l^2 + \beta_l\,\mathrm{e}^{-\sigma_l}\cos p_l$$

$$- \Lambda_{ll} \left(\frac{1}{2\sqrt{\pi} R_l} - \frac{\sqrt{2}\lambda_l \, \mathrm{e}^{-\eta}}{\sqrt{\pi}\sqrt{R_l^2 + R_j^2}} \right),$$

where $\sigma_l = 1/2R_l^2 + \delta_l^2 R_l^2/8$, $\eta = 2\chi^2/(R_l^2 + R_j^2)$, with $\chi = \xi_l - \xi_j$ is the distance between the mass centre of the two condensates. The formula $\chi \neq 0$ means that the two condensates are partially overlapped. The equations of motion of collective variables $\xi_l(t)$, $R_l(t)$, $p_l(t)$, and $\delta_l(t)$ are respectively given by

$$\begin{aligned}
\dot{p}_l &= \frac{2\sqrt{2}\lambda_l \Lambda_{ll} \, \mathrm{e}^{-\eta} \chi}{\sqrt{\pi}(R_l^2 + R_j^2)^{3/2}}, \\
\dot{\xi}_l &= \frac{\beta_l}{2} \, \mathrm{e}^{-\sigma_l} \sin p_l, \\
\dot{\delta}_l &= \beta_l \, \mathrm{e}^{-\sigma_l} \cos p_l \left(\frac{2}{R_l^4} - \frac{\delta_l^2}{2} \right) + \frac{\Lambda_{ll}}{\sqrt{\pi} R_l^3} \\
&\quad + \frac{2\sqrt{2}\lambda_l \Lambda_{ll}(1 - 4\eta) \, \mathrm{e}^{-\eta}}{\sqrt{\pi}(R_l^2 + R_j^2)^{3/2}}, \\
\dot{R}_l &= \frac{1}{2} \beta_l R_l \delta_l \, \mathrm{e}^{-\sigma_l} \cos p_l. \qquad (4)
\end{aligned}$$

Then the effective Hamiltonian of the l-th component becomes

$$\begin{aligned}
H_l &= -\beta_l \, \mathrm{e}^{-\sigma_l} \cos p_l + \frac{\Lambda_{ll}}{2\sqrt{\pi} R_l} \\
&\quad + \frac{\sqrt{2}\lambda_l \Lambda_{ll} \, \mathrm{e}^{-\eta}}{\sqrt{\pi}\sqrt{R_l^2 + R_j^2}}. \qquad (5)
\end{aligned}$$

The effective mass of the l-th component is $1/M_l^* = \partial^2 H_l / \partial p_l^2 = \beta_l \, \mathrm{e}^{-\sigma_l} \cos p_l$. It is clear that β_l and p_l significantly modify the effective mass M_l^*. Equation (5) indicates that the dynamical properties of the l-th component of the condensate are closely related to the parameters Λ_{ll}, λ_l, and the initial momentum p_{l0}. As discussed in Refs. [12]–[14], when $\cos p_{l0} > 0$, equation (4) presents a self-trapped state if $\Lambda_{ll} > \Lambda_{llc}$, otherwise, diffusion takes place if $\Lambda_{ll} < \Lambda_{llc}$. One can easily obtain

$$\Lambda_{llc} = \frac{2\sqrt{\pi}\beta_l \cos p_{l0} \, \mathrm{e}^{-1/2R_{l0}^2}}{R_{l0}^{-1} + 2\sqrt{2}\lambda_l \, \mathrm{e}^{-\eta_0}(R_{l0}^2 + R_{j0}^2)^{-1/2}}, \qquad (6)$$

where $\eta_0 = 2\chi_0^2/(R_{l0}^2 + R_{j0}^2)$, $\chi_0 = \xi_{l0} - \xi_{j0}$, $\sigma_{l0} = 1/2R_{l0}^2 + \delta_{l0}^2 R_{l0}^2/8$, ξ_{l0} and R_{l0} are the centre and width of the initial wave packet of l-th component, respectively.

When $\cos p_{l0} < 0$, the effective mass M_l^* is negative, indicating that the system has rich dynamics: self-trapping ($\Lambda_{ll} > \Lambda_{llc}$), stable moving soliton ($\Lambda_{ll} = \Lambda_{lls}$) and breather. Then we obtain[12–14]

$$\Lambda_{llc} = \frac{2\sqrt{\pi}\beta_l |\cos p_{l0}| (\varsigma - \mathrm{e}^{-1/2R_{l0}^2})}{R_{l0}^{-1} + 2\sqrt{2}\lambda_l \, \mathrm{e}^{-\eta_0}(R_{l0}^2 + R_{j0}^2)^{-1/2}}, \qquad (7)$$

where $\varsigma = \cos p_l / \cos p_{l0}$. And

$$\Lambda_{lls} = \frac{2\sqrt{\pi}\beta_l |\cos p_{l0}| \, \mathrm{e}^{-1/2R_{l0}^2}}{R_{l0} + 2\sqrt{2}\lambda_l R_{l0}^4 (R_{l0}^2 + R_{j0}^2)^{-3/2}} \qquad (8)$$

with $\chi_0 = 0$ in Eq. (4). Equations (6)–(8) are the key results obtained in this paper. Clearly, because of the admixture of the second component λ_l, the critical values Λ_{llc} for occurrences of the self-trapping, moving soliton/breather will be changed dramatically.

We now discuss the stability of the soliton solution (8). Setting $\delta_l = \delta_{l0} + \delta_l'$, $R_l = R_{l0} + R_l'$, and linearizing Eq. (4) near the soliton state, we have

$$\left[\dot{\delta}_1' \;\; \dot{\delta}_2' \;\; \dot{R}_1' \;\; \dot{R}_2' \right]^{\mathrm{T}} = J \left[\delta_1' \;\; \delta_2' \;\; R_1' \;\; R_2' \right]^{\mathrm{T}}, \qquad (9)$$

where J is the Jacobi matrix and its elements depend on Λ_{ll}, R_l and λ_l (see the Appendix). The eigenvalues of matrix J determine the stability of the soliton state. For simplicity, we consider the case of $R_{10} = R_{20} = R_0$, then the eigenvalues of J satisfy

$$\gamma^2 = \frac{\Lambda_{ll}^2 (1 + \lambda_l)^2}{\pi^2 R_0^2} (-1 + R_0^{-2}).$$

It is clear that when $\lambda_l \neq -1$, $\gamma^2 < 0$, i.e., the soliton state corresponds to an elliptic point and there is a stable moving soliton in this case. When $\lambda_l = -1$, however, the Jacobi matrix J only has zero eigenvalues, the soliton state corresponds to a neutral-stable point. In this case, the soliton state is likely to be stabilized in 1D optical lattices. In addition, we notice that when $\lambda_l = -1$, equation (8) (with $R_{10} = R_{20} = R_0$) is satisfied only when $p_{l0} = 0.5\pi$. Indeed, by the direct numerical simulations of Eq. (2), it is confirmed that this stable moving soliton state of the two-component BECs can certainly exist in 1D optical lattices.

As an example, figure 1 shows the critical value Λ_{11c} versus χ_0 (the initial distance between the mass centres of the two-component condensates) for different inter-component atoms interaction parameter λ_1. Clearly, Λ_{11c} strongly depends on λ_1, χ_0 and p_{10}. For example, for a fixed p_{10} and $\lambda_1 \neq 0$, Λ_{11c} increases with χ_0, and is continuously close to the critical value of the single-component case ($\lambda_1 = 0$) when $\chi_0 \to R_{10} + R_{20}$ and, finally, almost turns into the critical value of the single-component case completely when $\chi_0 \geq R_{10} + R_{20}$, at which the two-component condensates have no spacial overlap. Thus, we can conclude that for a fixed λ_1, the smaller the spatial overlap between the two-component condensates is (large χ_0), the more difficult it is for the system to

be self-trapped. In addition, when there is no overlap between the two components ($\chi_0 > R_{10} + R_{20}$), the dynamics of each component are similar to that of the single-component BEC. For a fixed χ_0 ($\chi_0 < R_{10} + R_{20}$), Λ_{11c} decreases with increasing λ_1, especially for small χ_0 (large spacial overlap between two condensates). In addition, the diffusive single-component condensate can be self-trapped with a minor admixture of the second component, even if the two condensates are only partially overlapped ($\chi_0 \neq 0$).

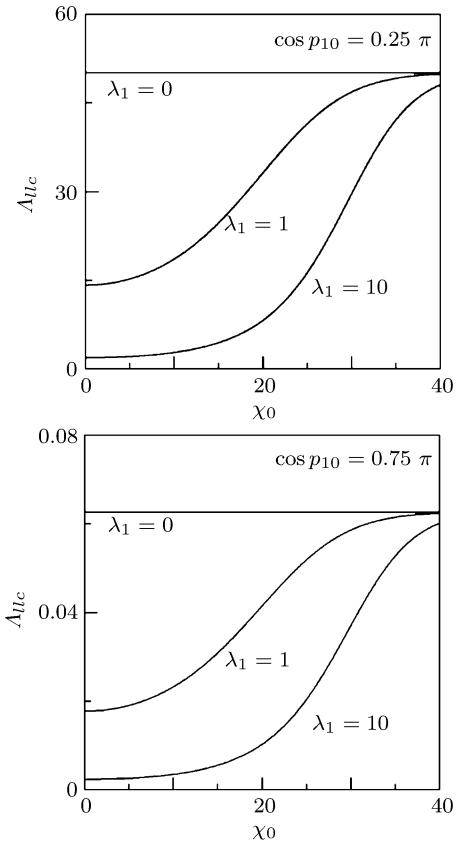


Fig. 1. The critical value Λ_{11c} of the two-component self-trapped state against χ_0 for different inter-component atom interaction parameters λ_1, with $R_{10} = 20$, $R_{20} = 10$.

4. Direct numerical simulations

To provide a further insight into the dynamics of the two-component BECs, we present some numerical simulations of the discrete GPE Eq. (2).

Figure 2 shows the self-trapped state of the two-component condensates. It is clear that when $\Lambda_{11} = 1.5 > \overline{\Lambda}_{11c} = 0.06$ (where $\overline{\Lambda}_{11c}$ is the critical value of the single-component), the single-component condensate ($\lambda_l = 0$) is self-trapped, but its life time is temporary (Fig. 2(a)). However, if there is an inter-component interaction ($\lambda_l = 1$) due to the admixture of another same component, a long-term self-trapped state will be realized (Fig. 2(b)). Furthermore, the self-trapped state of the primary-condensate, i.e., ^{87}Rb, can also be achieved due to an admixture of the minor-impurity component, i.e., ^{41}K (Fig. 2(c)), even if the mass centres of the two components are only partially overlapped (Fig. 2(d)). The above facts reveal that the self-trapped state is more easily realized with the minor admixture of the second component.

Figure 3 presents the moving breather state of the two-component BECs. When $\Lambda_{11} = 0.12 \simeq \overline{\Lambda}_{11s} = 0.125$ ($\overline{\Lambda}_{11s}$ is the critical value of the single component's soliton state), the amplitude of the moving wave packet almost remains a constant for the single component ($\lambda_l = 0$), corresponding to the stable moving soliton (Fig. 3(a)). But this stable moving soliton state will be broken down and becomes a moving breather state due to an admixture of another same component ($\Lambda_{11} = 0.12 > \Lambda_{11s} = 0.06$, Λ_{11s} is the critical value of the two-components' soliton state, Fig. 3 (b)). What is more, this situation also occurs with a minor admixture of the second different component, i.e., ^{87}Rb (the primary-component) and ^{41}K (the second-component), see Fig. 3(c), even if the mass centres of the two components are only partially overlapped (Fig. 3(d)), which enriches the results of Eq. (8) ($\chi_0 = 0$). However, the breather state will vary with the change of the two components overlapping.

Figure 4 shows the moving soliton state of the two-component BECs. Certainly, the moving soliton state can be easily realized if there is an inter-component interaction ($\lambda_l = 1$) due to an admixture of the second-component, even if for the single-component diffusive state ($\lambda_l = 0$, $\Lambda_{11} = 0.0585 < \overline{\Lambda}_{11c} = 0.06$), see Figs. 4(a) and 4(b). Moreover, if we continue to increase Λ_{11}, the moving soliton state still exists, even if the mass centres of the two components are only partially overlapped (Figs. 4(c) and 4(d)), which enriches the results of Eq. (8) ($\chi_0 = 0$).

As discussed in Section 3, when $R_{10} = R_{20}$, $\lambda_l = -1$ and $p_{l0} = 0.5\pi$, the stable moving soliton exists. To confirm this prediction, figure 5 shows the time evolution of the moving 1D wave packet with $R_{l0} = 20$, $p_{l0} = 0.5\pi$. When $\Lambda_{ll} = 0.05$, the single-component wave packet ($\lambda_l = 0$) is diffused with time (Fig. 5(a)). However, if there is an admixture of the second component and $\lambda_l = -1$, the stable moving soliton of the two-component condensate is achieved (Fig. 5(b)). So does the case for $\Lambda_{ll} = 5$ (the self-trapped state becomes the soliton state), see Figs. 5(c) and 5(d).

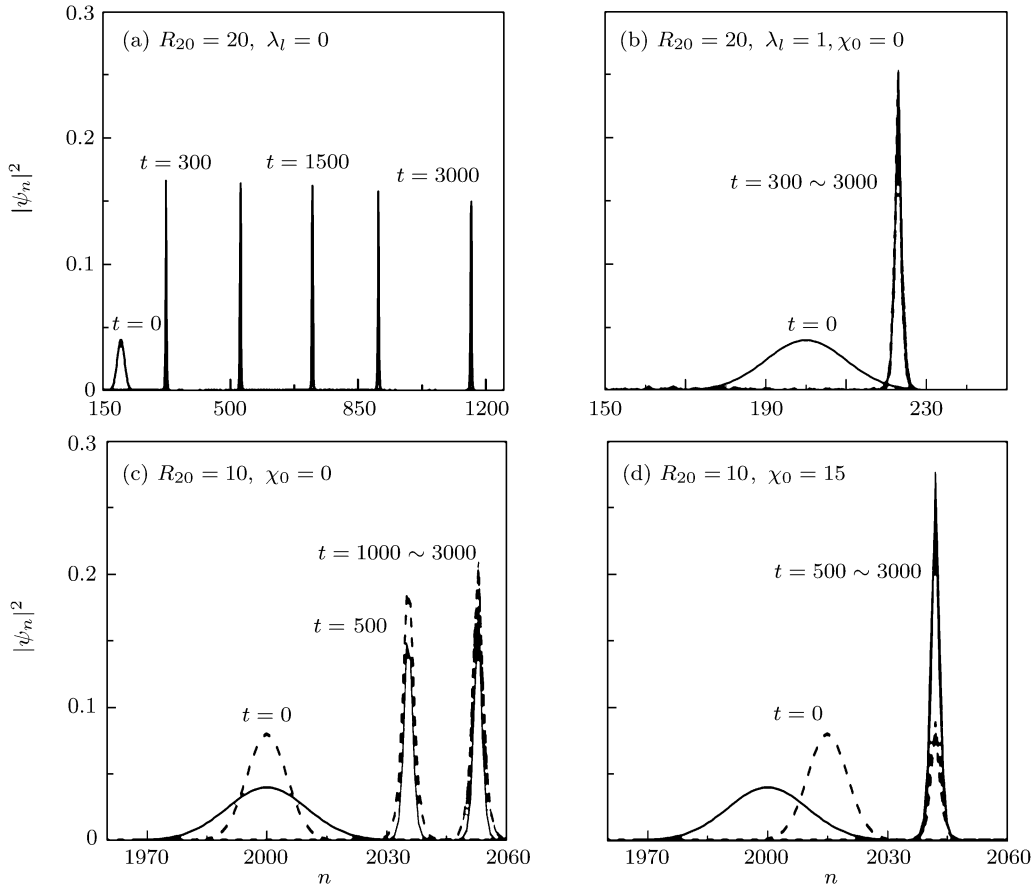


Fig. 2. Time evolution of the moving 1D wave packet with $\Lambda_{11} = 1.5$, $R_{10} = 20$, $p_{10} = 0.75\pi$: in panels (a) and (b), $\Lambda_{22} = 1.5$, $p_{20} = 0.75\pi$ for the same component; in panels (c) and (d): $\Lambda_{22} = 0.975$, $p_{20} = 2.8$, $\lambda_1 = 1.1$, $\lambda_2 = 2.5$ for two different components (^{87}Rb and ^{41}K). The short dashed line represents the second component.

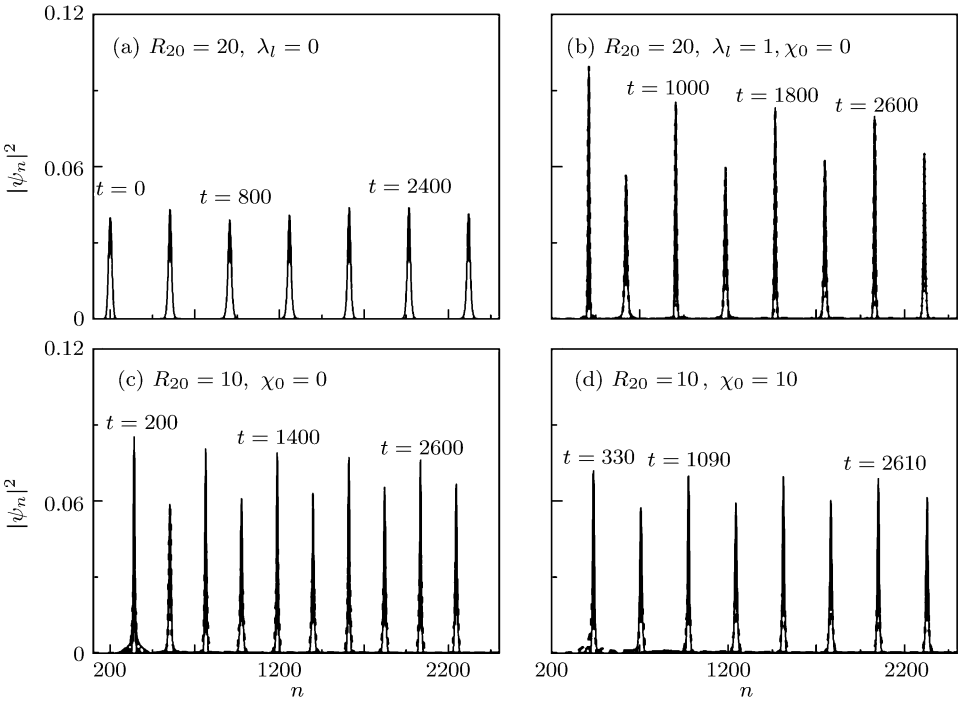


Fig. 3. Time evolution of the moving 1D wave packet with $R_{10} = 20$, $\Lambda_{11} = 0.12$, $p_{10} = 0.75\pi$, $\chi_0 = 0$; in panels (a) and (b), $\Lambda_{22} = 0.12$, $p_{20} = 0.75\pi$ for the same component; in panels (c) and (d), $\Lambda_{22} = 0.144$, $\lambda_1 = 2.1$, $\lambda_2 = 1.4$, $p_{20} = 2.8$ for two different components (^{87}Rb and ^{41}K). The short dashed line represents the second component.

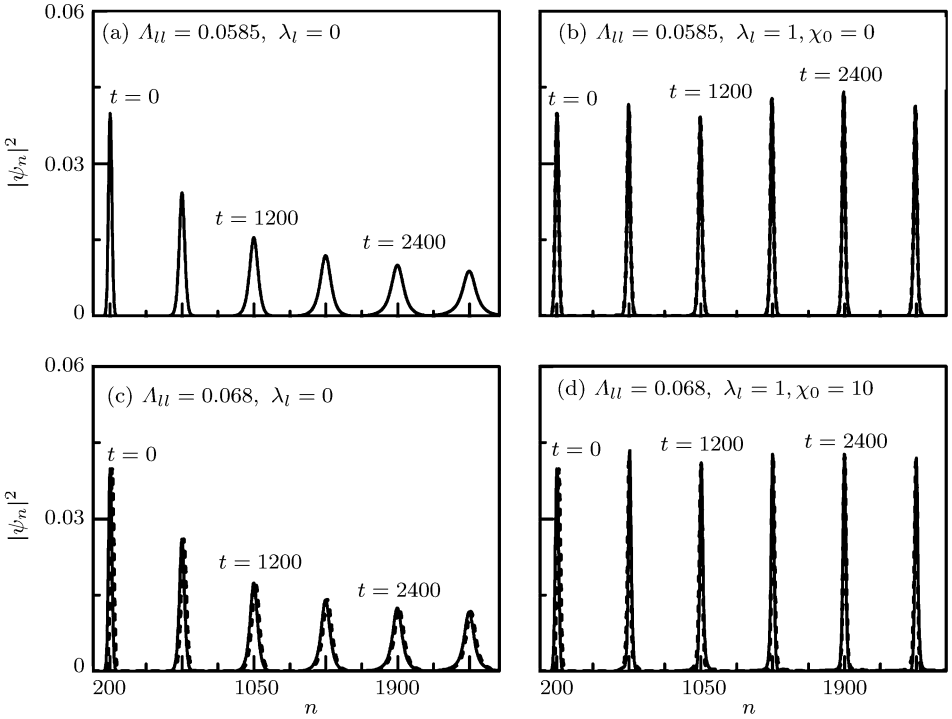


Fig. 4. Time evolution of the moving 1D wave packet with $R_{l0} = 20$, $p_{l0} = 0.75\pi$. The short dashed line represents the second component.

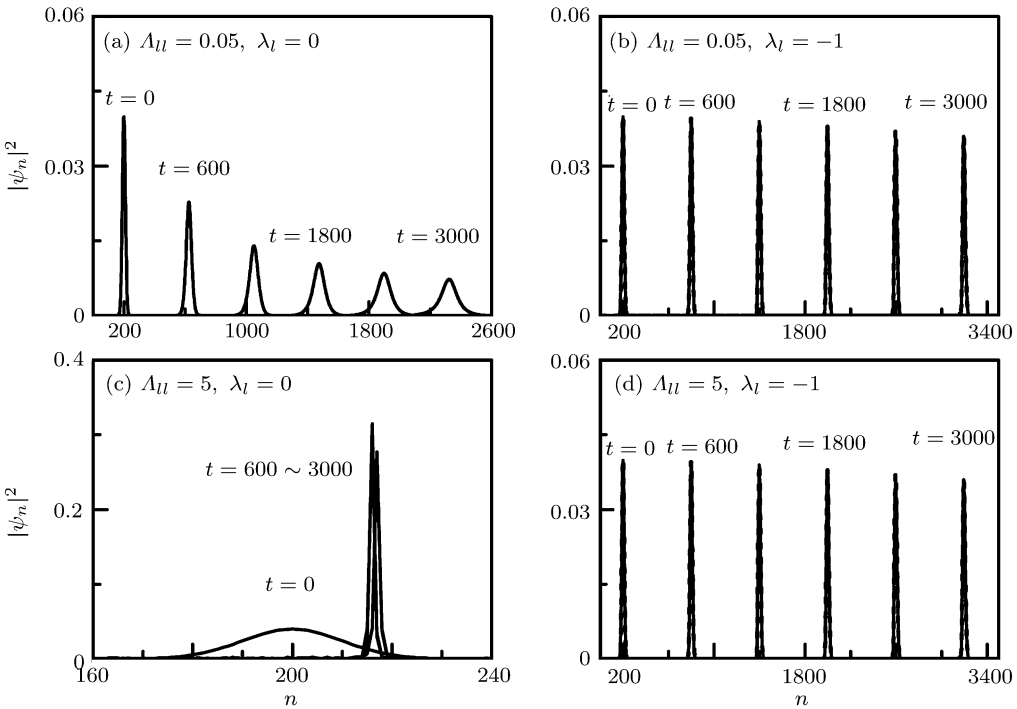


Fig. 5. Time evolution of the moving 1D wave packet with $R_{l0} = 20$, $p_{l0} = 0.5\pi$, $\chi_0 = 0$. The short dashed line represents the second component.

5. Conclusion

In summary, the role of the impurity component in the localization of two-component BECs loaded into deep 1D optical lattices is investigated both numerically and analytically. The criteria for occurrences of self-trapping and the moving soliton/breather of the primary-component condensates are obtained. Because of an admixture of the impurity-component, occurrences of self-trapping and the moving soliton/breather of the primary component become easier.

Appendix

The elements of the Jacobi matrix in Eq. (9) are given below

$$
\begin{aligned}
J_{13} &= \frac{\Lambda_{11}}{\sqrt{\pi}}\left[\frac{1-R_{10}^{-2}}{R_{10}^4}+2\sqrt{2}\lambda_1\frac{4-R_{10}^{-2}-3R_{10}^2(R_{10}^2+R_{20}^2)^{-1}}{R_{10}(R_{10}^2+R_{20}^2)^{3/2}}\right],\\
J_{14} &= -\frac{\Lambda_{11}}{\sqrt{\pi}}\frac{6\sqrt{2}\lambda_1 R_{20}}{(R_{10}^2+R_{20}^2)^{5/2}},\\
J_{23} &= -\frac{\Lambda_{22}}{\sqrt{\pi}}\frac{6\sqrt{2}\lambda_2 R_{10}}{(R_{10}^2+R_{20}^2)^{5/2}},\\
J_{24} &= \frac{\Lambda_{22}}{\sqrt{\pi}}\left[\frac{1-R_{20}^{-2}}{R_{20}^4}+2\sqrt{2}\lambda_2\frac{4-R_{20}^{-2}-3R_{20}^2(R_{10}^2+R_{20}^2)^{-1}}{R_{20}(R_{10}^2+R_{20}^2)^{3/2}}\right],\\
J_{31} &= -\frac{\Lambda_{11}R_{10}^5}{4\sqrt{\pi}}\left[R_{10}^{-3}+\frac{2\sqrt{2}\lambda_1}{(R_{10}^2+R_{20}^2)^{3/2}}\right],\\
J_{42} &= -\frac{\Lambda_{22}R_{20}^5}{4\sqrt{\pi}}\left[R_{20}^{-3}+\frac{2\sqrt{2}\lambda_2}{(R_{10}^2+R_{20}^2)^{3/2}}\right],
\end{aligned}
$$

and the other elements of J are all zero.

References

[1] Modugno G, Ferrari G, Roati G, Brecha R J, Simoni A and Inguscio M 2001 *Science* **294** 1320

[2] Zhang K Z, Wang J J, Liu G R and Xue J K 2010 *Acta Phys. Sin.* **59** 39 (in Chinese)

[3] Bai X D, Liu R H, Liu L, Tang R A and Xue J K 2010 *Acta Phys. Sin.* **59** 7581 (in Chinese)

[4] Morise H, Tsurumi T and Wadati M 2000 *Physica* A **281** 432

[5] Ieda J, Miyakawa T and Wadati M 2004 *Phys. Rev. Lett.* **93** 194102

[6] Greier M, Mandel O, Esslinger T, Hansch T and Bloch I 2002 *Nature* **415** 39

[7] Bartenstein M, Altmeyer A, Riedl S, Jochim S, Chin C, Denschlag J Hecker and Grimm R 2004 *Phys. Rev. Lett.* **92** 120401

[8] Bourdel T, Khaykovich L, Cubizolles J, Zhang J, Chevy F, Teichmann M, Tarruell L, Kokkelmans S J J M F and Salomon C 2004 *Phys. Rev. Lett.* **93** 050401

[9] Günter K, Stoferle T, Moritz H, Kohl M and sslinger T E 2006 *Phys. Rev. Lett.* **96** 180402

[10] Ospelkaus S, Ospelkaus C, Wille O, Succo M, Ernst P, Sengstock K and Bongs K 2006 *Phys. Rev. Lett.* **96** 180403

[11] Catani J, De Sarlo L, Barontini G, Minardi F and Inguscio M 2008 *Phys. Rev.* A **77** 011603 (R)

[12] Wang J J, Zhang A X, Zhang K Z, Ma J and Xue J K 2010 *Phys. Rev.* A **81** 033607

[13] Xue J K, Zhang A X and Liu J 2008 *Phys. Rev.* A **77** 013602

[14] Xue J K and Zhang A X 2008 *Phys. Rev. Lett.* **101** 180401